SSRG International Journal of Civil Engineering
ISSN: 2348-8352/ https://doi.org/10.14445/23488352/IJCE-V13I9P113

Volume 13 Issue 9, 217-238, September 2026

Original Article

Experimental Evaluation of the Fresh and Hardened State Performance of Flowable Concrete Reinforced with Pineapple Leaf Fiber (PALF)

Mabel Liz Zevallos Cruz[1], Angel Anibal Almerco Yalico[1], Alí Pompeyo Rivera Leiva[1], Giancarlo Fernando Meza Terbullino[1*]

[1]*School of Civil Engineering, Universidad Continental, Huancayo, Peru.*

[*]*Corresponding Author : gmezat@continental.edu.pe*

Received: 02 June 2026 Revised: 02 September 2026 Accepted: 18 September 2026 Published: 29 September 2026

Abstract - *Conventional concrete exhibits brittle behavior under tensile and flexural stresses, which promotes crack initiation and may reduce its durability. The incorporation of natural fibers such as pineapple leaf fiber represents a promising alternative for improving the mechanical performance of concrete. In this study, an experimental approach was used to evaluate the influence of four Pineapple Leaf Fiber (PALF) dosages-0.2%, 0.4%, 0.6%, and 0.8% by weight of cement-on flowable concrete, compared with a control mixture under equivalent cement and water contents. Fresh-state performance was assessed through slump, unit weight, air content, slump-flow, J-Ring, and L-box tests, while hardened-state performance was evaluated through compressive, splitting tensile, and flexural strength tests at 7 and 28 days. The results showed that the 0.6% PALF dosage provided the best overall balance between fresh-state performance and mechanical resistance, increasing compressive strength by 22.32% and splitting tensile strength by 37.42% at 28 days compared with the control mixture. Although the 0.8% dosage produced the highest flexural strength, it also caused a marked reduction in flowability and passing ability. Therefore, a PALF dosage of 0.6% was identified as the most favorable overall condition within the evaluated range.*

Keywords - *Flowable concrete, Pineapple Leaf Fiber (PALF), Natural fibers, Fresh-state properties, Hardened-state properties, Workability, Compressive strength, Flexural strength, Sustainable concrete, Fiber-reinforced concrete.*

1. Introduction

Concrete is one of the most widely used construction materials because of its high durability, availability, and ease of production. Despite these advantages, it presents a brittle behavior response under tensile and flexural stresses, which facilitates crack initiation and propagation.

Fig. 1 Cracking appearing on the road pavement [3]

These cracks affect structural stability and shorten the project's lifespan [1, 2]. Structures are subjected to loads, vibrations, and service conditions which cause the eventual formation of cracks; the reports of road works evidence that continuous crack propagation can ultimately compromise the structural integrity and reduce the service time.

Consequently, developing mixes with enhanced mechanical properties and improved crack control is an important research line in civil engineering. Figure 1 shows a road pavement that exhibits cracking, highlighting the need for developing mixes with enhanced mechanical properties [3].

Recent studies have shown that incorporating fibers in concrete can enhance post-cracking behavior and ductility; mechanical properties such as tensile and flexural strength are also improved [4]. The fibers act as bridging elements, which limits the propagation of cracking after the initial crack. Specifically, natural fibers have received special attention given their low cost, high availability, renewable source, and because they are eco-friendliness compared to synthetic fibers [5].

The Pineapple Leaf Fiber (PALF) presents favorable mechanical properties and can potentially serve as reinforcement in cementitious materials. However, the effect of fibers on concrete depends on the type, fiber-matrix bond, and dosage; the use of small dosages can enhance the tensile and flexural strength and at the same time, the crack control. In contrast, excessive dosage is related to a workability reduction, dispersion difficulties, and negatively effects on compressive strength [6, 7]. Previous studies have confirmed that PALF can modify both the fresh and hard concrete behaviour [8]. Regarding the self-compacting approach [9], the PALF contains of 0,2 %, 0,3 % and 0,4 % were evaluated considering the weight of the concrete, and these reported dependent changes on dosages of the performance in a fresh state through the usage of slump and flow tests, V-funnel, and L-box, along with variations In the strength and flexural resistance in the 7 and 28 days.

The biggest strength resistance is the compression, where a PALF of 0.3% was obtained, while the biggest flexural resistance was registered with a PALF of 0.4%. These findings demonstrate that a simultaneous evaluation of the properties of the fresh and hard concrete with a high workability reinforced with PALF was performed. Hence, this current study does not look for being the first PALF evaluation in both states; but this research looks for expanding research about low dosages of up to 0.8% and apply a broader experimental matrix for examining the relationship between fresh-state mobility, passing mobility and mechanical performance [10, 11].

Natural fibers have gained much more attention as reinforcement for cementing materials because of their mechanical, economical and environmental potential, especially as renewable alternatives for synthetic fibers. [12]. Recent investigations like [13] evaluated reinforced concrete with pineapple leaves employing fiber contains of 1 %, 2 %, 3 % and 4 %, and identified that the 2 % dosage is the one that has the best performance. The experimental program considered workability, density, compressive strength, splitting tensile strength, and flexural strength. Also, the SEM and EDX analysis were employed for examining the microstructural characteristics and the matrix-fiber interaction, while the economical and environmental evaluations considered the cost of production and the CO_2 emissions. These findings bring a broader perspective about mechanical, microstructural, and sustainability implications related to the incorporation of PALF. Nonetheless, the evaluation of the fiber content in [13] was higher than the researched one in this study. The performance of natural fibers in the concrete is also strongly influenced by the features of the fibers and their interaction with the cementing matrix because their physical and chemical properties can affect both the mechanical answers and the workability [14]. As a consequence, the findings of Hasan et al. Provide an important complementing point of reference for comprehending the depending behavior of dossification of reinforced concrete with PALF.

It is known that steel, polypropylene, coconut, and sisal fibers have shown improvements in the main properties of concrete in different studies. Each of them has different characteristics. Steel fiber provides better mechanical response, polypropylene has low density and good stability against water, while coconut and sisal fibers are related to the reuse of organic materials, although they can reduce workability [15, 16]. In this context, the contribution of this current study lies in the evaluation PALF within a range of 0,2% and 0,8% dosages in the cement weight, keeping equivalent contents of cement and water in all of the mixes. The experimental matrix integrates settlement measurements, unit weight, air content, settlement-fluency, J-ring and L-box, along with compressive resistance, splitting tensile, and flexural strength tests at 7 and 28 days. This designs amplifies the low dosage ranges of PALF previously evaluated [9] and permitted to examine the evolution of mobility in a fresh state and passing mobility altogether with mechanical properties. Thus, the novelty of this investigation is defined by the specific dosage interval and the integrated experimental evaluation, in comparison with the first PALF incorporation in high-workability concrete.

This research has the aim to experimentally evaluate the performance of fresh-state and hard-state fluid concrete reinforced with PALF within the dosage range of 0,2 and 0,8% in the cement weight. The study examines, specifically, the influence of PALF content in the workability and weight capacity, along with the along with compressive, splitting tensile, and flexural strength at 7 and 28 days. These experimental mixtures are compared with control mixtures that have an equivalent content of cement and water. The aim is to identify the PALF dosage that gives a general balance that is the most favorable between the performance in the fresh state and mechanical resistance.

2. Materials and Methods

A comparative and experimental approach is carried out. The control mix of the flowable concrete and four PALF-reinforced mixtures in proportions of 0.2%, 0.4%, 0.6%, and 0.8% by weight of cement are evaluated. Then, the resulting specimens' properties are tested in fresh (comparing workability and density) and hardened state (compressive, splitting tensile, and flexural strengths).

2.1. Materials

2.1.1. Cement

The Portland Type I was employed, according to the ASTM C150/C150M guideline [17], as a binder in all experimental mixtures. The cement was acquired commercially from a local distributor in Huancayo. This type of cement is destined to concrete application of general usage in which “especial properties” are not especificallt required, like a high initial resistance or a higher resistance to sulfates. According to [18]. Eh, Portland cement Type I often present a high composition in calcium, dominated by CaO and SiO_2, along with moderate content of Al_2O_3, Fe_2O_3, MgO and SO_3. The physical and chemical features of reference of the cement Portland Type I is summarized in Table 1. These values are presented as reference properties based on literature and not as direct results of the chemical characterization of the cement employed in the experimental program.

Table 1. Typical reference properties of Type I Portland cement

Property	Typical range	Mean reference value	Unit
SiO_2	18.7–22.0	20.5	%
Al_2O_3	4.7–6.3	5.4	%
Fe_2O_3	1.6–4.4	2.6	%
CaO	60.6–66.3	63.9	%
MgO	0.7–4.2	2.1	%
SO_3	1.8–4.6	3.0	%
Na_2O equivalent	0.11–1.20	0.61	%
$_3S$	40–63	54	%
C_2S	9–31	18	%
C_3A	6–14	10	%
C_4AF	5–13	8	%
Blaine fineness	300–421	369	m²/kg
Specific gravity	≈3.15	≈3.15	—

2.1.2. Aggregates

As fine aggregate, natural sand is used, and crushed stone as coarse aggregate, both sourced from a local quarry. The aggregates were characterized via a sieve analysis according to the ASTM C136 [19], and the specific gravity, absorption, and unit weight according to ASTM C127 [20], C128 [21], and C29 [22], respectively.

These procedures served to verify the suitability of the aggregates for producing conventional concrete, as shown in Table 2 and Figures 1 and 2 below.

Table 2. Physical properties of the aggregates used in the experimental mixtures

Property	Fine aggregate	Coarse aggregate	Standard/source
Material type	Natural sand	Crushed stone	Experimental material
Bulk specific gravity (OD)	2.569	2.685	ASTM C128 / ASTM C127
Bulk specific gravity (SSD)	2.579	2.693	Calculated from OD specific gravity and absorption
Apparent specific gravity	2.595	2.703	ASTM C128 / ASTM C127
Water absorption (%)	0.40	0.30	ASTM C128 / ASTM C127
Angularity (%)	31.20	92.80	Laboratory characterization
Los Angeles abrasion (%)	-	16.00	ASTM C131
Sand equivalent (%)	68.65	-	T176
Maximum aggregate size (mm)	-	25.0	Gradation result
Nominal maximum aggregate size (mm)	-	19.0	Gradation result

The combined gradation was separated in the 4,75 mm sieve, and then it was normalized for independently representing the fine and coarse aggregate fractions. The resulting curve distributions of size are depicted in Figure 2(a) and Figure 2(b), respectively. The fine fraction includes the range from 0,08 to 4,75 mm, while the coarse fraction is extended from 4,75 to 25,0 mm. The recovered gradation is consistent with the maximum aggregate size of 25,0 mm and a maximum nominal aggregate size 19,0 mm. These distributions are employed for documenting the aggregate skeleton adopted in the mix design, while the proportions of reported materials were kept for all of the experimental mixtures.

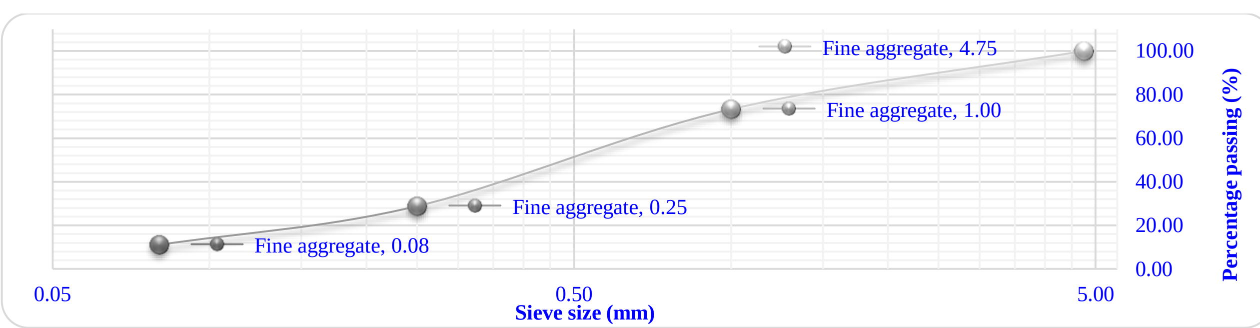

(a)

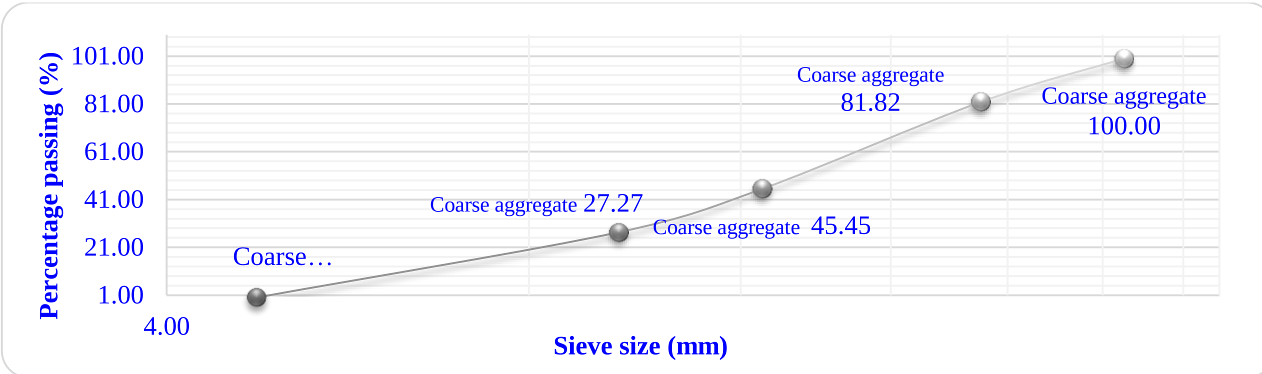

(b)

Fig. 2 (a) Grading curve for fine aggregate, and (b) Grading curve for coarse aggregate.

2.1.3. Pineapple Leaf Fiber (PALF)

The utilized PALF in the experimental mixtures was prepared with a nominal length of approximately 50 mm. Because of the extraction and preparation process, the fibers presented an irregular distribution of diameter, as displayed in Figures 3 and 4.

Fig. 3 Natural and processed pineapple fiber

Fig. 4 PALF extraction process

2.1.4. Superplasticizer

A commercially available water-reducing and fluidifying admixture (CHEMA SÚPER PLAST) is used. This water-reducing admixture is commonly used to produce high-performance concrete; the admixture complies with the ASTM C494 type A standard [23]. The admixture dosage is established based on the percentage by weight of cement, ranging from 1% to 2.10% and following the workability requirements of the experimental design. The admixture is incorporated diluted in the mixing water to ensure adequate dispersion in the concrete mix.

2.1.5. Water

Potable water free of impurities is used, according to the requirements for concrete mixtures of the ASTM C1602 standard [24].

2.2. Experimental Design

2.2.1. Characterization and Preparation of PALF Fiber

The nominal length of the PALF fiber of 50 mm was adopted for all of the experimental mixtures, following the geometry of the fiber described by Abisha and Nalanth [25], for the self-compacting concrete with PALF. In this reference, a diameter of approximately of 0,5 mm of fiber was informed, and an aspect rate of 100. These geometric parameters were solely considered as “reference value” based on literature and were not obtained through the dimensional direct characterization of PALF employed in this study.

Also, tensile strength ranging from approximately 180 to 753 MPa for PALF were reported, depending on the pineapple variety and the extraction procedure [8]. The extraction procedure and preparation for PALF adopted in this research was based on previously described methods for residual papers of comosus ananas, in which the papers are subjected to conditioning and to a non-fiber material separation for recovering usable longitudinal fibers [26].

In this current study, no chemical or microstructural characterization direct from PALF were performed. Hence, related parameters like the chemical composition, superficial morphology, fiber diameter, and the relationship between the aspect and the tensile strength were only considered as reference information based on literature and should not be represented like direct characterization results of the fibers employed in the experimental program. FTIR, SEM either EDX analyses were not performed.

Previous studies have demonstrated that superficial characteristics and physical properties of PALF can vary according to the extraction and conditioning procedure [8]. As a consequence, any interpretation related to the matrix-fiber interaction, fiber union, or morphological effects are analyzed in reference to previous studies, instead of treating them as direct microstructural evidence obtained in this current research.

2.2.2. PALF Dosage

The PALF dosage range was selected based on the content intervals of fibers reported in previous experimental studies and the need to evaluate the progressive answer of the mixtures of a relatively low dosage range.

According to Hendrian [9], who investigated PALF contents of 0,2 %, 0,3 % and 0,4 % in cement weight in self-compacting concrete, demonstrating that even low fiber contents can modify both the behavior and the mechanical performance of the concrete in the fresh state.

On the contrary, [13], evaluations with a higher dosage of 1 %, 2 %, 3 % and 4 % of PLF and reported a progressive workability reduction as more fiber content increased, observing that the best overall performance with an intermediate dosage.

Base don these previous ranges, this current study adopted PALF contents of 0,2 %, 0,4 %, 0,6 % and 0,8 % in cement weight. The increase of 0,2 percentual points gave a systematic sequence for evaluating the evolution of the properties in fresh and hard state, while the superior limit of 0,8% extended the low content range previously investigated by [9], without reaching fiber contents that were substantially higher, which were examined by Hasan et al.

Hence, this experimental interval permitted to progressively evaluate the relationship between PALF dosage, fluency, passing capacity, and mechanical resistance under equivalent content of water and cement. The adopted mixture closed, and the PALF contents are in the summary Table 3.

Table 3. Mixture nomenclature and PALF dosage

Mixture code	PALF dosage by weight of cement
PALF-0	0.0 %
PALF-0.2	0.2 %
PALF-0.4	0.4 %
PALF-0.6	0.6 %
PALF-0.8	0.8 %

2.2.3. Mixing Procedure

The Mixing procedure follows the ASTM C192/C192M standard [28]; this standard dictates guidelines for the preparation of concrete specimens in the laboratory. Figure 5 shows a flowchart of the specimen preparation; the procedure begins by weighing materials and ends with casting with molds. Figure 6 shows the concrete mix (as part of the homogeneity verification step) in the fresh state and the PALF dispersion, before the mold casting step.

The mixture design was established from a reference mixture without fiber, designed to reach a specified compressive strength of f'c = 210 kg/cm². These proportions were considered according to the criteria established by ACI 211.1 [29].

According to this standard, the concrete mixture must meet the required strength, workability, and material characteristics. The pineapple leaf fiber (PALF) was added to the concrete mixture according to the cement content, without changing the cement amount, as shown in Table 4.

Table 4. Concrete dosage with PALF

Mixture	Cement (kg/m³)	Water (kg/m³)	Fine Aggregate (kg/m³)	Coarse Aggregate. (kg/m³)	PALF (kg/m³)
PT	350	192.5	760	1050	0.00
PALF 0.2 %	350	192.5	760	1050	0.70
PALF 0.4 %	350	192.5	760	1050	1.40
PALF 0.6 %	350	192.5	760	1050	2.10
PALF 0.8 %	350	192.5	760	1050	2.80

This methodology made it possible to directly evaluate the progressive influence of PALF on the fresh and hardened properties of concrete, while keeping the cementitious matrix under equivalent conditions.

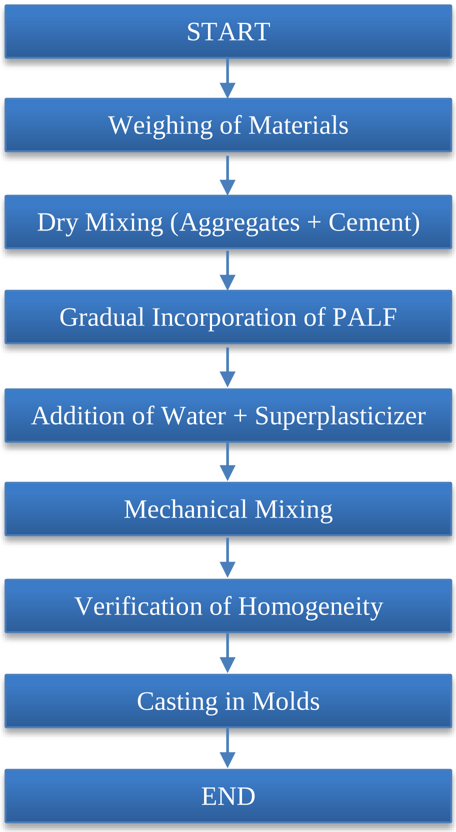

Fig. 5 Specimens' preparation flowchart

Fig. 6 PALF-reinforced concrete mix in the fresh state

2.2.4. Casting and Curing of Specimens

The ASTM C192 standard dictates the rules for specimens' preparation in the laboratory [28]. In this context, the specimens are demolded after 24 h, and then they are cured in water at a constant temperature (23°C ± 2 °C). Testing ages of 7 and 28 days are considered.

2.3. Fresh State Tests

In this current study, the term «cluid concrete » refers to a concrete mix with high workability that is produced with a water reducer additive of high amplitude and that was evaluated according to its capacity to extend and go through confined armour conditions. The term is employed intentionally instead of classifying all the mixes as Self-Compacting Concrete (SCC), because the experimental mixes showed different capacity passing levels as the PALF content increased. Thus, the Slump-flow, J-Ring, and L-box tests were used because these are commonly utilized in the SCC, like complementary indicators for quantifying the flow and passing capacity without restrictions, and for determining how the PALF content affected these features when in a fresh state.

2.3.1. Slump Test

The slump test is carried out according to the ASTM C143 standard [30]. This standard test describes the procedure to measure the consistency of fresh concrete. The slump cone is filled with three layers compacted by rodding. Subsequently, the mold is lifted vertically, and the height loss of the concrete is measured in mm. This test evaluates the influence of PALF and the superplasticizer on the workability and consistency of fresh concrete.

2.3.2. Unit Weight Determination

The unit weight of fresh concrete is determined by following the ASTM C138 standard [31], which requires the use of a calibrated measure of a known volume. The concrete is placed in layers and compacted by rodding, then it is struck off and weighed. For the unit weight calculation—which is defined as the ratio between fresh concrete mass and volume of the calibrated measure— Equation 1 is used. This test evaluates the density variations because of the addition of PALF in the mix and the effects of entrapped air.

$$\rho = \frac{m}{V} \tag{1}$$

Where:

- ρ = unit weight (kg/m³)
- m = fresh concrete mass (kg)
- V = volume of the calibrated measure (m³)

2.3.3. Air Content

The air content is used to evaluate the entrapped air in the mix and its effects on the density and mechanical properties of concrete. An increase in air content can decrease the strength or enhance the workability of the mix. The test is conducted according to the ASTM C231 [32] and NTP 339.080 [33] standards, which dictate the use of a pressure method where the air content is determined based on the movement of air inside a measuring bowl. Specifically, the fresh concrete is placed in a bowl in three layers of equal volume, and then each layer is compacted by rodding. Subsequently, the bowl is sealed, and a controlled pressure is applied, as result the air content is measured by a manometer.

The calculation of air content can be done using Equation (1), which provides a way of determining the effect of PALF on the entrapped air of the mix and its relation with compaction and voids.

2.3.4. Complementary Workability Test

Given the fact that the usage of a reductor additive in high-range water produced mixtures with high fluency, it was not considered that the conventional slump test would be enough alone for characterizing the behaviour during the fresh state. Therefore, additional flow-slump tests, J-Ring, and L-bo were performed for evaluating the non-confined flow and the passing capacity. These tests are commonly used for self-consolidating concrete; however, in this current study, these tools were applied as diagnosis tools for quantifying the PALF effect over mobility and susceptibility to obstruction of fluid mixtures.

Slump Flow

The aim of the slump flow test is to evaluate the flowability and deformability of concrete in the fresh state. This is especially relevant to high-flowability mixes as a consequence of the superplasticizer. The test also permits the characterization of concrete that does not require compaction, which is the case of self-compacting concrete or high-workability concrete. The procedure is carried out according to the ASTM C1611/C1611M standards [34]; the use of a flat, rigid, and non-absorbent surface is mandatory.

In addition, the mold is filled in a single lift and then lifted vertically to allow a free spread. Subsequently, two perpendicular diameters are measured; the average spread diameter or slump flow is calculated using the two measured diameters as shown in Equation (2). Based on the diameter difference values, the test is repeated if the difference between the two diameters exceeds 50 mm, in order to obtain reliable results. Ultimately, these values are an indicator of the flowability of the mixes that considers the effect of PALF in lowering the expansion capacity.

$$SF = \frac{d_1 + d_2}{2} \quad (2)$$

Where:

- SF: average spread diameter
- d_1 and d_2 : measured perpendicular diameters

J-Ring Test

By using the J-Ring test, the passing ability of concrete in the fresh state is measured. This is useful to simulate the concrete behavior in confined structures and allows us to identify the blocking or segregation problems in high-flowability mixtures, especially after the incorporation of PALF. The aforementioned procedure is conducted according to the ASTM C1621/1621M standard [35]; the mold is placed concentrically in the J-Ring that contains reinforcing bars. Lastly, the uncompacted concrete is poured to allow free flow.

To calculate the J-Ring flow diameter (SFJ), the perpendicular diameters of the final extension of concrete are measured. Equation (3) shows the SFJ definition; The difference between the slump flow diameter (SF) and the J-Ring flow (SFJ) diameter were employed as indicators of the passing capacity. According to the ASTM C1621/C1621M guidelines, the differences inferior to 25 mm indicate a good passing capacity, while the differences superior to 50 mm indicate a deficient passing capacity. The intermediate values indicate a growing trend towards the block. These criteria were employed in the current study with the purpose to interpret the PALF dosage effect over the mixture capacity to flow through a simulated reinforcement congestion. The adopted criteria is summarized in Table 5.

$$SFJ = \frac{d_1 + d_2}{2} \quad (3)$$

Where:

- SFJ = J-Ring flow diameter (mm)
- d_1 and d_2: measured perpendicular diameters (mm)

Table 5. Blocking evaluation criteria

Difference (SF − SFJ)	Interpretation
0–25 mm	No visible blocking
25–50 mm	Minimal to noticeable blocking
>50 mm	Severe blocking

L-Box Test

To evaluate the passing ability and flowability of concrete in confined conditions, the L-Box test is employed; this simulates the behavior through elements with reinforcement congestion. In addition, the test allows the identification of blocking or loss of homogeneity problems that are present in high-workability mixes. The procedure is conducted following the EN 12350-10 standard [36]. An L-box apparatus (that consists of a vertical and horizontal section that are separated by a sliding gate) is used, in which the uncompacted concrete is poured.

Subsequently, the concrete flows freely through reinforcing bars. In the testing, the heights of concrete before and after the flow are recorded. Based on these data, the passing ability ratio (PA) is calculated as the ratio between the final height of the concrete in the horizontal section and the initial height of the concrete in the vertical section, as it is shown in equation (4). The L-box passing capacity was utilized ($PA = H_2/H_1$) for evaluating the concrete capacity in order to flow through the confined armour. In this research, a PA value $PA \geq 0,80$ was adopted as an acceptance threshold for an adequate passing capacity, while values inferior to 0,80 are interpreted as hints of a growing block or mobility loss. This criterion is used for identifying the PALF dosage from which the passing capacity during the fresh state starts to deteriorate.

$$\boldsymbol{PA} = \frac{\boldsymbol{H_2}}{\boldsymbol{H_1}} \quad (\mathbf{4})$$

Where:

- PA = passing ability ratio
- H_1 = initial height of concrete in the vertical section (mm)
- H_2 = final height of concrete in the horizontal section (mm)

2.4. Hardened State Tests

2.4.1. Compressive Strength Test

The compressive strength test is used to evaluate the resistance under axial loads, which is a key mechanical property in structural design. The test can also provide information about the influence of PALF in concrete in the hardened state. The ASTM C39 [37] and NTP 339.034 [38] standards are used; the previously prepared and cured specimens (under controlled conditions) are used, after verifying the flatness and perpendicularity of their surface.

The specimens are subjected to a continuous axial load in a compression testing machine until failure, and the maximum load before failure is measured. The compressive strength is calculated as the ration between the maximum applied load and the cross-sectional area of the specimen, as depicted in Equation (5). The tests are conducted at the ages of 7 and 28 days, which allows the evaluation of strength development and the comparison between different dosages and the control mixture.

$$f'c = \frac{Pmax}{A} \quad (5)$$

Donde:

- $f'c$ = compressive strength (MPa)
- Pmax = maximum applied load (N)
- A = Cross-sectional area of the cylinder (mm^2)

2.4.2. Splitting Tensile Strength Test

The splitting tensile test was used to evaluate the tensile strength of the concrete and the influence of PALF on its response to indirect tensile loading. The test provides a resistance indicator of the cementing matrix for the splitting tensile, but it does not characterize the subsequent behavior after the cracking directly. According to the ASTM C496/C496M guidelines [39], the cured test specimens were placed horizontally in bearing plates of the test machine. Later, the axial load was applied along the specimen until failure due to diametral cracking occurred, and the maximum load applied was registered. The splitting tensile strength was calculated by employing Equation(6).

$$ft = \frac{2P}{(\pi LD)} \quad (6)$$

Donde:

- ft = splitting tensile strength (MPa)
- P = maximum applied load applied by the testing machine (N)
- L = length of the specimen (mm)
- D = diameter of specimen (mm)

2.4.3. Flexural Strength Test

The flexural strength test is used to evaluate concrete behavior under tensile stresses that are present in the bottom surface of an element subjected to transverse loads. This test determines the concrete resistance to cracking; this is relevant when concrete is implemented in structural elements, especially for the fiber-reinforced concrete case. The procedure for the test is conducted according to the ASTM C78 standard [40], the standard dictates the use of prismatic specimens under a third-point loading. The specimens are placed on simple supports and are loaded at two equidistant points.

During the tests, a continuous load was applied until failure, and the maximum load was registered. The modulus of rupture was calculated based on the maximum load, the span length, and the cross-sectional dimensions of the specimen, as it is depicted in equation (7). These results were employed for evaluating the influence of PALF dosage in the flexural maximum resistance and the rupture modulus of the concrete mixtures. The post-cracking behavior, residual resistance, flexural toughness, and energy absorption were not directly evaluated in the present experimental program.

$$MR = \frac{PL}{bd^2} \quad (7)$$

Where:

- MR = modulus of rupture (MPa)
- P = maximum applied load applied by the testing machine
- L = span length (mm)
- b = average width of the specimen at the fracture (mm)
- d = average depth of the specimen at the fracture (mm)

Statistical Analysis

The results of compressive strength, indirect tensile strength, and flexural strength splitting tensile strength using a two-way factorial analysis of variance (ANOVA). The independent factors will be the PALF content (0, 0.2, 0.4, 0.6, and 0.8%) and the curing age (7 and 28 days), including the PALF × age interaction.

On the other hand, the experimental variability and repeatability of the mechanical test results will be expressed as mean ± Standard Deviation (SD), calculated from the different dosages used with PALF fiber and the curing age.

3. Results

3.1. Slump and Air Content in the Mixture without Superplasticizer

The results of the slump test indicated that as the PALF dosage increases and without the addition of superplasticizer, the slump decreases from 74 to 49 mm that fresh mixture tends to become dry (< 2”), as shown in Figure 7. These outcomes indicated that PALF progressively reduced the consistency of the mixtures when a superplasticizer was not utilized. As a consequence, a water-reduction additive of high range was required for obtaining the necessary fluency level for subsequent assessments of settlement and trafficability.

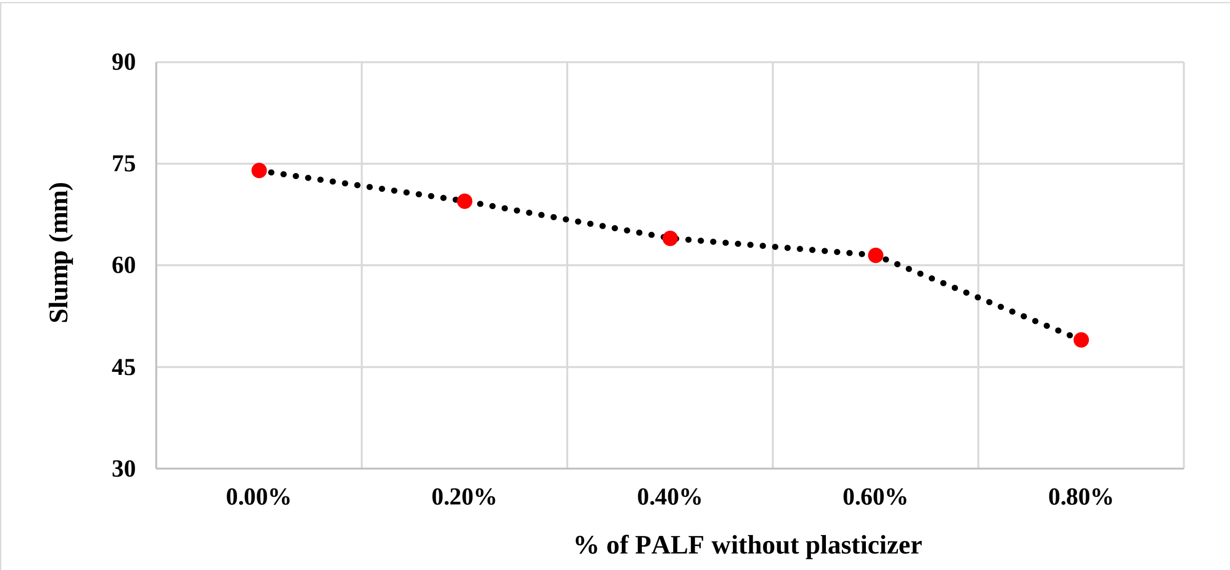

Fig. 7 Slump test results for different dosages of PALF without the addition of a superplasticizer

Figure 8 depicts the air content for every dosage of PALF without considering the superplasticizer. It can be observed that air content decreases, which is attributed to fiber rearrangement, reducing the interconnected voids. However, when PALF content exceeds 0.6%, the air content increases, as is the case for 0.8%.

Fig. 8 Air content for different dosages of PALF without the addition of a superplasticizer

3.2. Slump Flow

Figure 9 shows the slump flow test results for different dosages of PALF and including superplasticizer. As PALF content increases (up to 0.6%) the slump flow decreases by an average of 1.9%. This value is obtained based on the difference between consecutive dosages. Specifically, the reduction from the control mixture to PALF0.2% is 2.03%, for PALF0.2% with respect to PALF0.4% is 2.19%; and finally, from PALF0.4% to PALF0.6% is 1.62%. When the dosage increases to 0.8% it is noted a decrease in slump of 5.9% with respect to the 0.6% mixture. This value is calculated analogously to the previous comparisons.

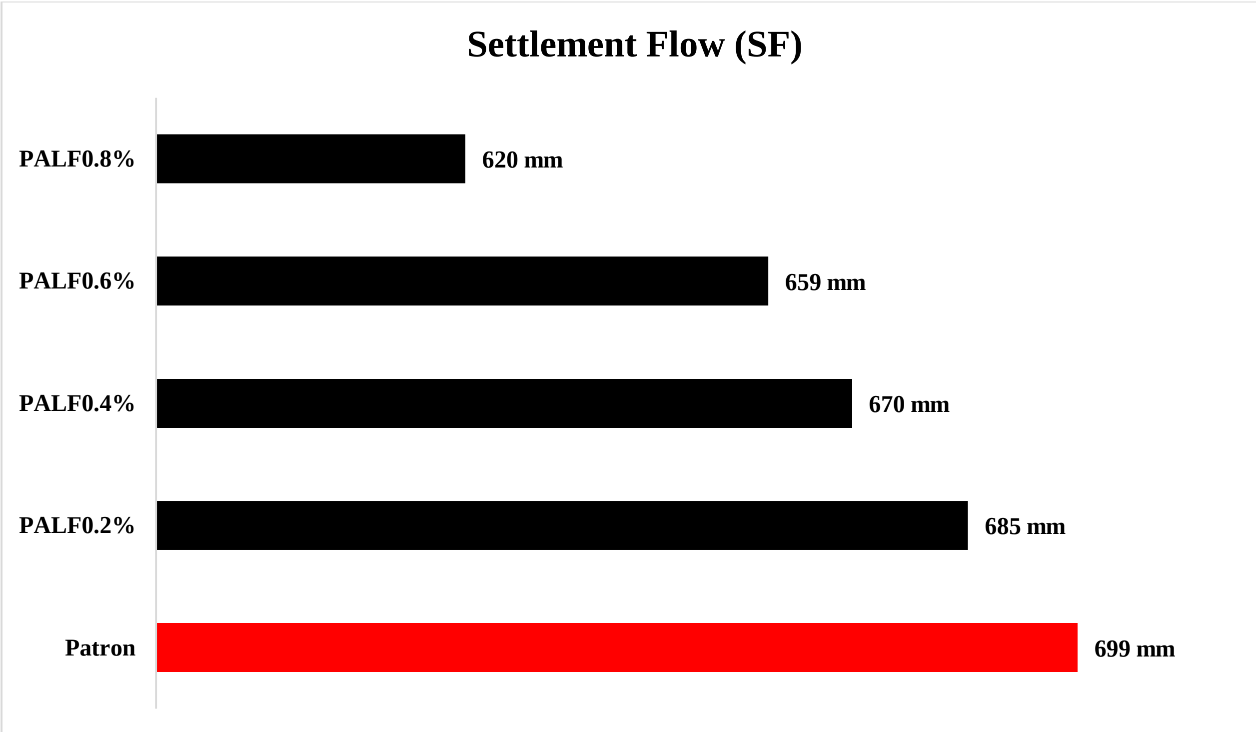

Fig. 9 Slump flow results for different PALF dosages

3.3. Passing Ability Test

Figure 10 shows the passing ability results for different dosage proportions of PALF, considering the addition of superplasticizer. It can be seen that for different ranges of PA, a corresponding blocking category is assigned. PALF dosages in the range of 0–0.4% correspond to no visible blocking. In contrast, the PALF dosage of 0.6% evidences a minimal to noticeable blocking range, as shown in Figure 10.

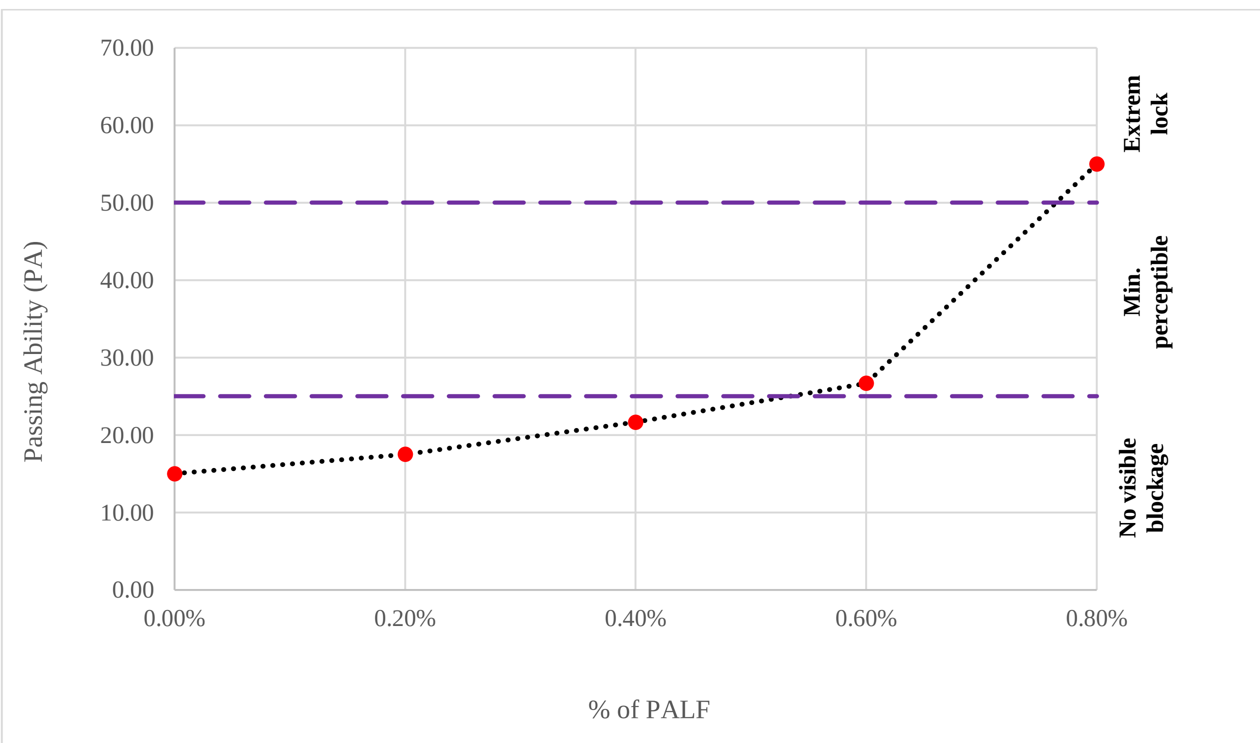

Fig. 10 PA for different dosages of PALF

Fig. 11 PA test verification

3.4. L-Box Test

Figure 11 shows the passing ability results for different PALF dosages, which consider the addition of superplasticizer and the acceptance or rejection criteria. The PALF dosages in the range of 0–0.4% evidenced an acceptable behavior (PA>0.8); the PALF0.6% case represents a threshold case, as beyond that, the PA value (PALF0.8% case) decreases by 53.7% compared to the control mixture. Figure 12 shows the L-Box test.

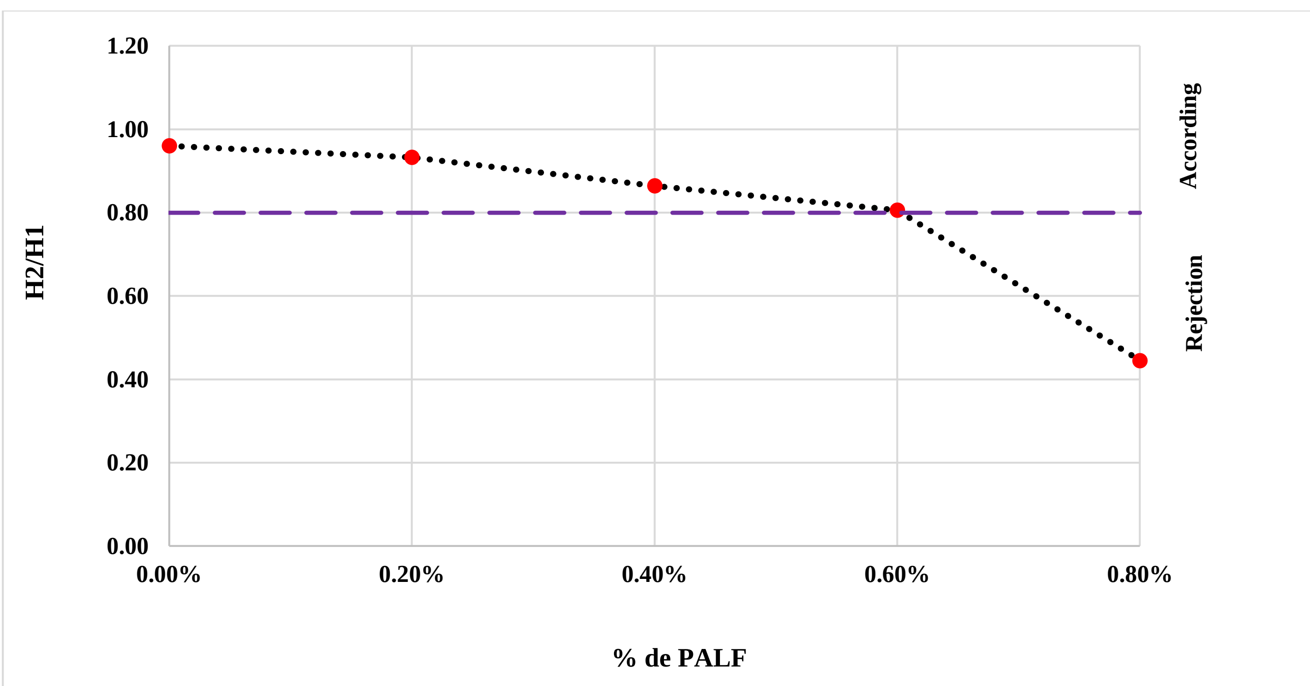

Fig. 12 PA test results for different PALF dosages

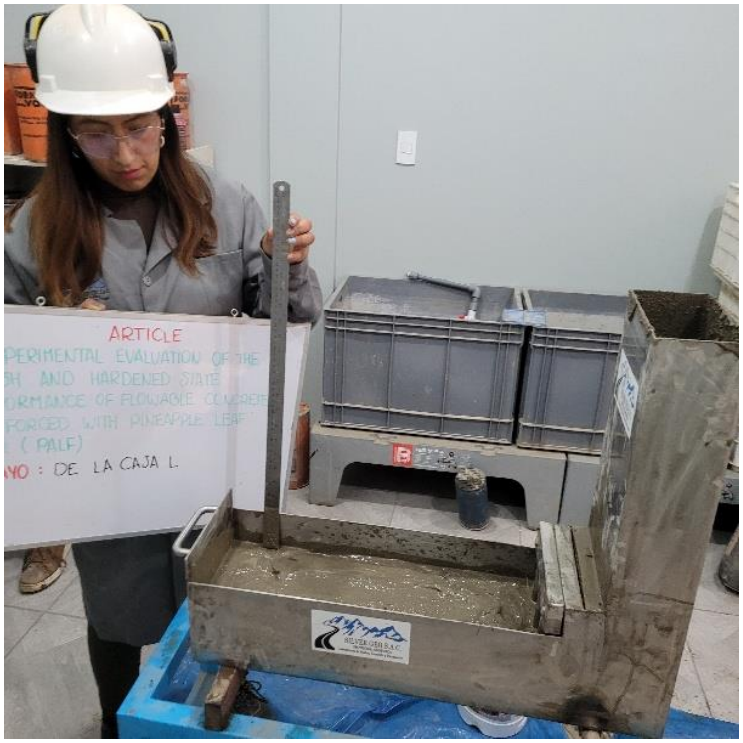

Fig. 13 L-Box test

3.5. Compressive Strength

Figure 13 shows the compressive strength test results of specimens at 7 and 28 days, and for different PALF dosages. The 7-day specimens that included PALF showed an increase in compressive strength compared to the design strength; the specimen with a PALF proportion of 0.6% evidenced the highest increase in compressive strength compared to the control specimen, with a value of 13.45%. In a similar way, the 28-day specimens also evidenced an increase in compressive strength. Analogously, the PALF0.6% evidenced the highest increase in compressive strength relative to the control specimen, 22.32%. Figure 14 shows the compressive strength test.

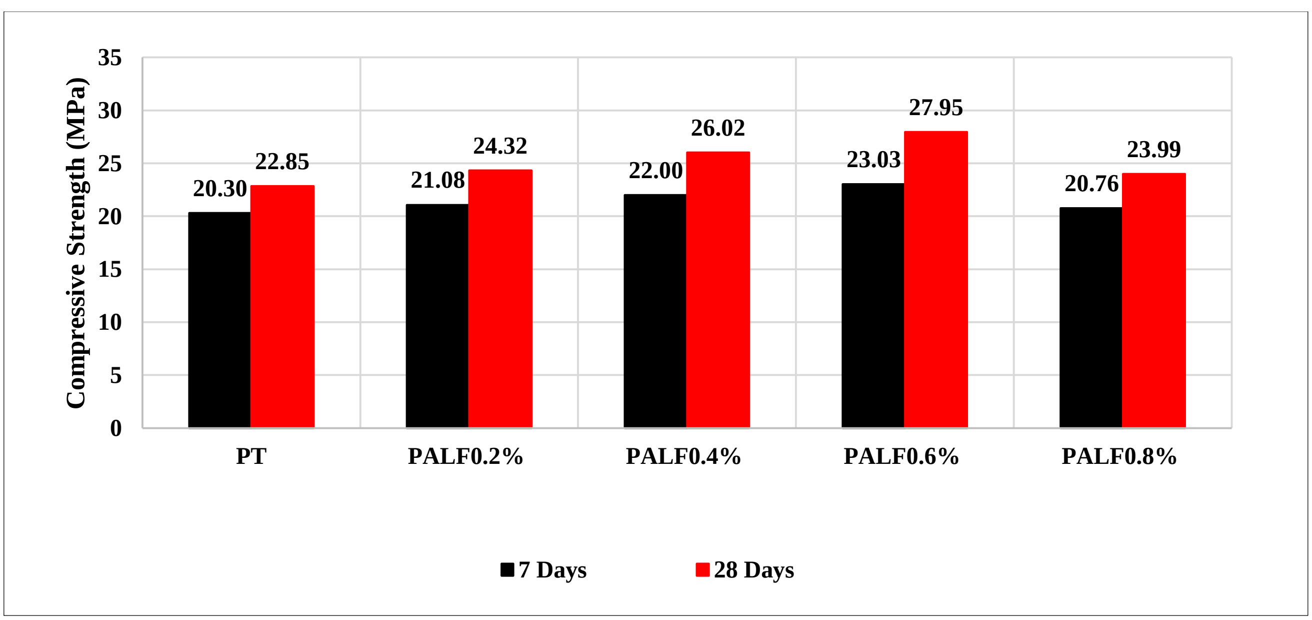

Fig. 14 Compressive strength test results across different PALF dosages

Fig. 15 Compressive strength test

3.6. Splitting Tensile Strength

Figure 16 depicts the splitting tensile strength test results carried out in specimens at 7 and 28 days, and at different PALF dosages. The 7-day specimens evidenced an increase in tensile strength relative to the control specimen; the PALF0.6% specimen presented the highest increase in tensile strength, 29.48%. Analogously, the 28-day specimens presented an increased tensile strength; the PALF0.6% specimen evidenced the highest increase in strength, 37.42%.

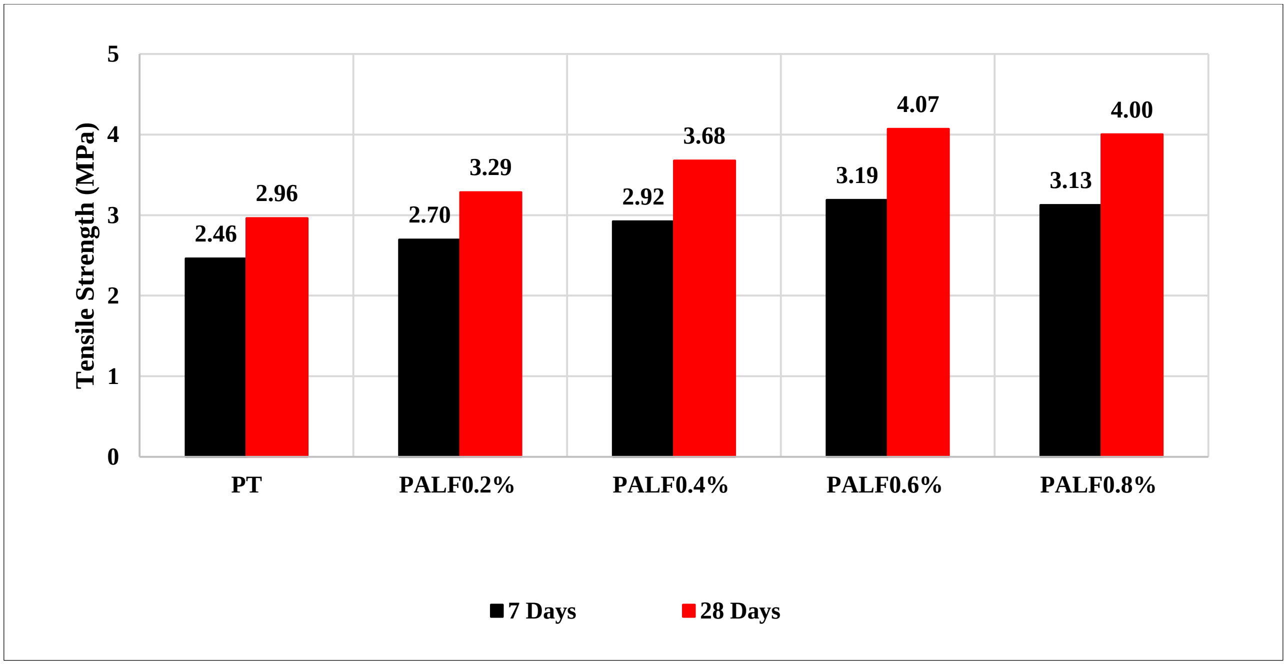

Fig. 16 Tensile strength results across different PALF dosages

3.7. Flexural Strength

Figure 17 illustrates the flexural strength test results that correspond to specimens at 7 and 28 days, and across different dosages of PALF. As with the other strength test results, all the mixtures presented an increase in flexural strength compared to the control mixture. In the flexural strength test, the PALF0.8% mixture presented the highest increase at 7 and 28 days, 23.32%, and 23.34%, respectively.

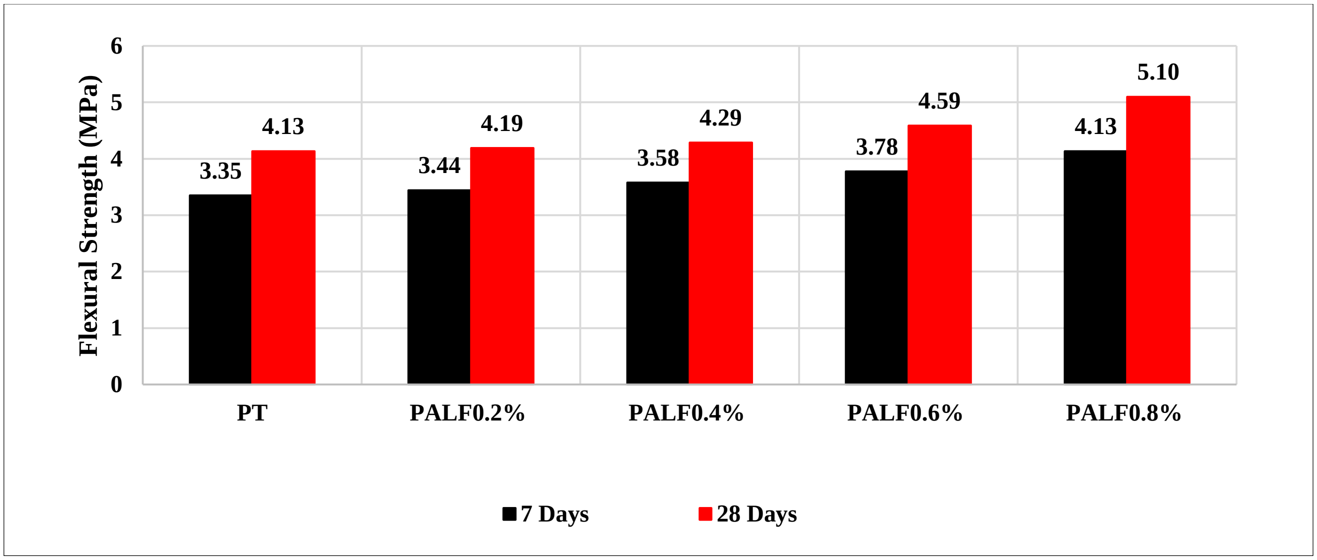

Fig. 17 Flexural strength test results

3.8. Box-Plot Diagrams

Figure 18 depicts a box-plot diagram for the mechanical resistance test. The compressive strength box-plot diagram at 7 and 28 days (as shown in Figure 18(a) and Figure 18(b)) highlights a gradual increase in compressive strength in the range of 0–0.6%, although at a dosage of 0.8%, the resistance decreased by 9.87% and 14.15% compared to the PALF0.6% specimen, at 7 and 28 days, respectively. Analogously, the tensile strength box-plots (in Figures 18(c) and Figure 18(d)) show that the PALF0.8% sample experienced a decrease of 1.95% and 1.69% compared to the PALF0.6% mixture. Finally, in the flexural strength box-plot diagram (depicted in Figure 18(e) and Figure 18(f)), a continuous increase in flexural strength is noted across all the range of PALF dosage, 0.2–0.8%.

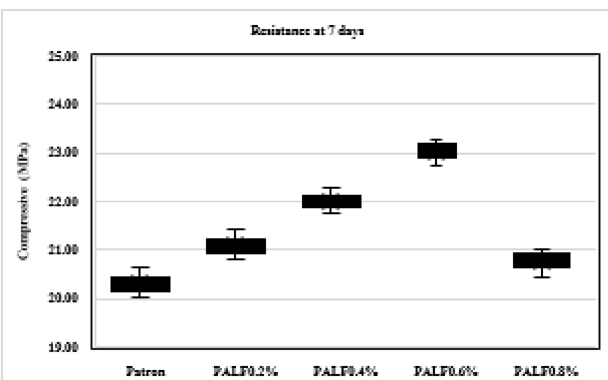

(a)

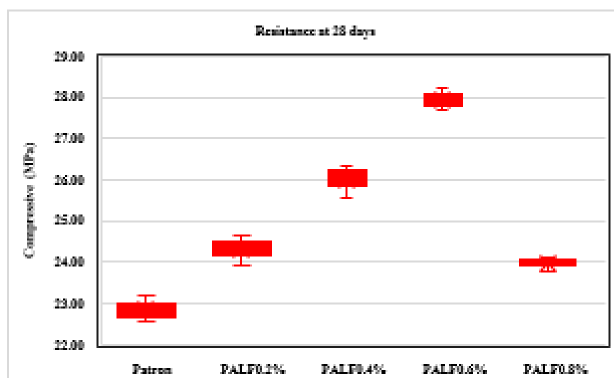

(b)

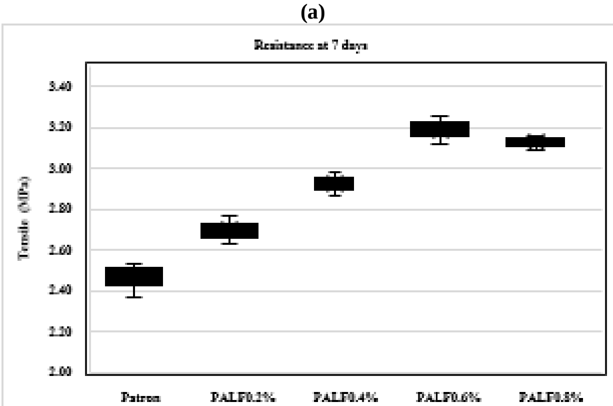

(c)

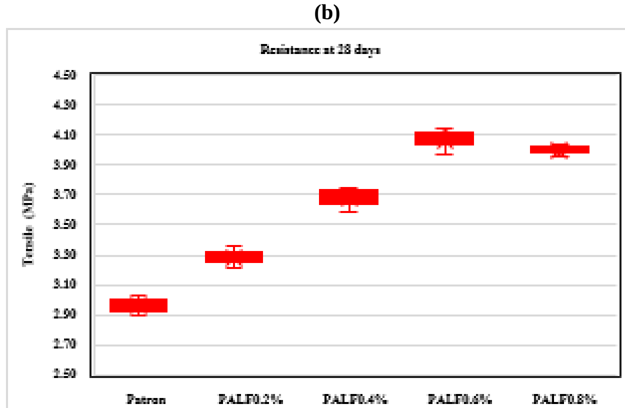

(d)

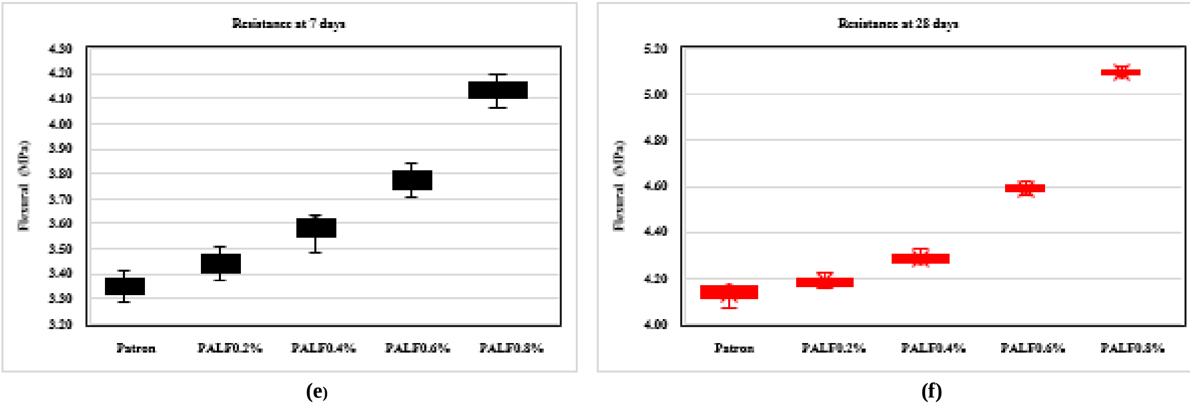

Fig. 18 Box-plot diagrams of the mechanical properties at different dosages and at 7 and 28 days

3.8.1. Statistical Analysis Results

To determine whether the observed variations in mechanical properties were statistically significant, a two-way Analysis of Variance (ANOVA) was performed. PALF dosage (0, 0.2, 0.4, 0.6, and 0.8%) and curing time (7 and 28 days) were considered fixed factors, including the interaction between PALF dosage and curing time. A significance level of $\alpha = 0.05$ was adopted. When statistically significant differences were identified, Tukey's HSD post hoc test was applied to perform multiple comparisons between experimental conditions. In addition to the F-statistic and p-value, degrees of freedom (df), sums of squares (SS), Mean Squares (MS), and partial eta-squared (ηp^2) were reported to provide a more comprehensive assessment of statistical significance and effect size. 95% confidence intervals for the experimental means were also determined. The complete ANOVA results are presented in Table 6.

For each combination of PALF dosage and curing time, three samples were evaluated for each mechanical property. The presented mean, standard deviation, coefficient of variation, and confidence intervals were calculated from these three sample-level measurements. The number of replicates remained constant across all PALF dosages and curing times, resulting in a balanced experimental design.

Table 6. Two-way ANOVA results for the mechanical properties

Property	Source	df	Sum of Squares (SS)	Mean Square (MS)	F	p-value	Partial η²
Compressive strength	PALF dosage	4	56.802	14.200	151.82	<0.001	0.968
	Curing age	1	96.768	96.768	1034.57	<0.001	0.981
	PALF × age	4	4.931	1.233	13.18	<0.001	0.725
	Error	20	1.871	0.094	-	-	-
Splitting tensile strength	PALF dosage	4	3.614	0.903	188.56	<0.001	0.974
	Curing age	1	3.888	3.888	811.54	<0.001	0.976
	PALF × age	4	0.173	0.043	9.00	<0.001	0.643
	Error	20	0.096	0.0048	-	-	-
Flexural strength	PALF dosage	4	3.010	0.753	237.58	<0.001	0.979
	Curing age	1	4.848	4.848	1530.63	<0.001	0.987
	PALF × age	4	0.060	0.015	4.73	0.008	0.486
	Error	20	0.063	0.0032	-	-	-

As shown in Table 6, PALF dosage and curing time had statistically significant effects on compressive strength, splitting tensile strength, and flexural strength ($p < 0.001$). The interaction between PALF dosage and curing time was also statistically significant for compressive strength and splitting tensile strength ($p < 0.001$), as well as for flexural strength ($p = 0.009$). Partial eta-squared (ηp^2) values further demonstrated that PALF dosage and curing time had pronounced effects on all three mechanical properties. The interaction between PALF dosage and curing time also showed a substantial effect on compressive and splitting tensile strengths, whereas its effect on flexural strength was comparatively smaller. These results indicate that the mechanical response to PALF incorporation varied depending on the curing time.

Three samples per experimental condition were used to assess the repeatability of the mechanical tests, while maintaining a consistent number of replicates across the experimental matrix. The relatively low coefficients of variation obtained for the mechanical properties indicate limited dispersion among replicate measurements. However, the use of three samples per condition represents a limitation of the statistical analysis, and future studies should consider a larger number of independent experimental replicates to enhance statistical robustness.

The normality of the ANOVA residuals was assessed using the Shapiro–Wilk test, whereas homogeneity of variances was evaluated using Levene's test. A significance level of $\alpha = 0.05$ was adopted for both assumption checks. Residual plots were additionally examined to identify systematic deviations or influential observations.

Table 7. Mean values and 95% confidence intervals at 28 days

PALF Dosage	Compression (MPa)	Indirect tensile strength (MPa)	Flexural strength (MPa)
0 %	22.85 (22.04–23.66)	2.96 (2.79–3.13)	4.13 (4.00–4.27)
0.2 %	24.32 (23.42–25.23)	3.29 (3.11–3.46)	4.19 (4.10–4.28)
0.4 %	26.02 (25.02–27.02)	3.68 (3.46–3.89)	4.29 (4.21–4.37)
0.6 %	27.95 (27.26–28.64)	4.07 (3.85–4.29)	4.59 (4.52–4.66)
0.8 %	23.99 (23.54–24.45)	4.00 (3.90–4.10)	5.10 (5.05–5.15)

As depicted in Table 7, the PALF mixture with 0,6% presented the highest exhibited the highest compressive and splitting tensile strengths at 28 days, while the PALF mixture with 0,8 % reached the highest flexural resistance. The average values, standard deviations, and variation coefficients for the compression resistance, splitting tensile and flexural strengths at the 7 and 28 days are presented in Tables 8, 9 and 10, respectively.

Table 8. Compressive strength results at 7 and 28 days

PALF	7 days, mean ± SD (MPa)	CV (%)	28 days, mean ± SD (MPa)	CV (%)
0 %	20.30 ± 0.312	1.54	22.85 ± 0.328	1.43
0.2 %	21.08 ± 0.306	1.45	24.32 ± 0.364	1.50
0.4 %	22.00 ± 0.270	1.23	26.02 ± 0.403	1.55
0.6 %	23.03 ± 0.274	1.19	27.95 ± 0.279	1.00
0.8 %	20.76 ± 0.288	1.39	23.99 ± 0.182	0.76

Table 9. Splitting tensile strength results at 7 and 28 days

PALF	7 days, mean ± SD (MPa)	CV (%)	28 days, mean ± SD (MPa)	CV (%)
0 %	2.46 ± 0.087	3.54	2.96 ± 0.069	2.32
0.2 %	2.70 ± 0.069	2.55	3.29 ± 0.069	2.09
0.4 %	2.92 ± 0.059	2.01	3.68 ± 0.087	2.37
0.6 %	3.19 ± 0.069	2.15	4.07 ± 0.087	2.14
0.8 %	3.13 ± 0.034	1.10	4.00 ± 0.039	0.98

Table 10. Flexural strength results at 7 and 28 days

PALF	7 days, mean ± SD (MPa)	CV (%)	28 days, mean ± SD (MPa)	CV (%)
0 %	3.35 ± 0.064	1.90	4.13 ± 0.054	1.31
0.2 %	3.44 ± 0.069	1.99	4.19 ± 0.035	0.84
0.4 %	3.58 ± 0.083	2.33	4.29 ± 0.032	0.74
0.6 %	3.78 ± 0.069	1.82	4.59 ± 0.029	0.64
0.8 %	4.13 ± 0.069	1.67	5.10 ± 0.020	0.40

Experimental variability was evaluated using the Standard Deviation (SD) and the Coefficient of Variation (CV), based on three samples for each combination of PALF dosage and curing age. The coefficients of variation ranged from 0.76% to 1.55% for compressive strength, from 0.98% to 3.54% for splitting tensile strength, and from 0.40% to 2.33% for flexural strength. These relatively low CV values indicate limited dispersion among the tested samples within each condition. Figures 14, 16, and 17 present the mean mechanical strength values with error bars corresponding to ±1 standard deviation to graphically represent the variability among measurements.

4. Discussion

The slump results in mixtures without superplasticizer evidenced a gradual decrease in workability as the PALF dosage increased; the decrease range was from 74 to 49 mm that corresponded to the increase of PALF from 0% to 0.8%, and indicated a tendency to dry mixtures. The same decrease in workability was reported in previous studies [9], in which increasing the PALF dosage in self-compacting concretes resulted in reduced flow diameter, directly affecting the deformability in the fresh state. A possible explanation is the high aspect ratio, the specific surface area, and the water absorption of the fibers; these factors increase the internal friction and decrease the flowability of the mixture.

The air content test evidenced a reduction in voids up to a PALF dosage of 0.6%; this was associated with the enhanced fiber distribution in the cementitious matrix. This behavior is aligned with previous studies [27], that indicated that low dosages of natural fibers can reduce the porosity. However, it was found that increasing the dosage up to 0.8% increases the air content; this is associated with the fiber agglomeration and creation of heterogeneous zones that are presented in high fiber contents [41].

The slump flow results that included the use of superplasticizer evidenced a gradual decrease in flowability up to a PALF dosage of 0.6% and an average decrease of 1.9% in successive applications. However, a high PALF dosage of 0.8% caused a 5.9% reduction in workability. Similarly, other studies of basalt fiber-reinforced concrete evidenced a gradual decrease in flowability as the fiber content increased [11]. A plausible explanation is the fiber entanglement and the increased internal resistance to flow; this phenomenon was reported in self-compacting concretes with fibers, in which high fiber content reduces the flowability, passing ability, and can cause blocking [42, 43].

Regarding the passing ability, the mixtures with a PALF dosage in the range of 0–0.4% did not evidenced visible blocking; the mixtures with a dosage of 0.6% and above evidenced a tendency to blocking. This can be explained by increased fiber-fiber and fiber-aggregate interactions, which increases the passing ability between objects. The same tendency was previously reported (expressed as the H2/H1 ratio in the L-Box test) when the fiber content was increased [44]. Another study indicated that a high fiber content increased viscosity and reduced flowability [45], which negatively affected the passing ability; this phenomenon is illustrated in Figure 18.

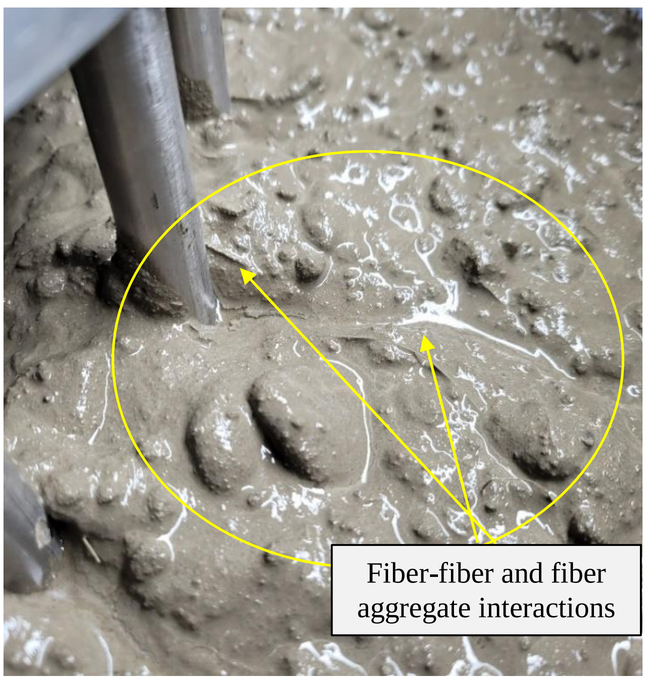

Fig. 19 Fiber-fiber and fiber-aggregate interactions

The compressive strength results evidenced a general increase in strength at both 7-day and 28-days specimens when PALF dosage was included, with respect to the control specimen. The highest performance was evidenced at the PALF0.6% specimen, which presented an increase of 13.45% and 22.32%, on the 7 and 28 days, respectively.

The increase in compressive strength observed at PALF contents of up to 0.6% may be linked to a better distribution of fibers within the cementitious matrix and their potential contribution to limiting the development of localized cracks. Similar mechanisms have been described in fiber-reinforced concrete, where fibers can act as bridges across forming cracks and facilitate stress transfer through the cementitious matrix [46]. In general, an adequate dosage of fibers can improve the mechanical performance of concrete in comparison with control mixtures [7]. However, since no direct microstructural characterization was performed in this study, the proposed mechanisms should be viewed as interpretations supported by the literature rather than direct experimental evidence of the fiber-matrix interaction. At a PALF dosage of 0.8%, compressive strength decreased compared to the 0.6% mix, although it remained higher than that of the control concrete. This reduction could be attributed to less efficient fiber distribution and the potential formation of heterogeneous zones at higher fiber contents, as reported in previous studies.

The splitting tensile strength results showed that the incorporation of PALF increased the tensile strength of all mixtures compared to the control concrete. The highest values were obtained with a PALF dosage of 0.6%, corresponding to increases of 29.48% and 37.42% at 7 and 28 days, respectively. This improvement is consistent with the fiber-bridging mechanism described in previous studies on fiber-reinforced concrete [47], in which fibers can contribute to stress transfer across developing cracks and, consequently, increase the measured tensile strength. However, the present study did not directly characterize fiber bridging through crack-width measurements or microstructural analyses; therefore, this mechanism is discussed as an interpretation supported by the literature rather than as directly observed experimental evidence. At a PALF dosage of 0.8%, the splitting tensile strength decreased slightly compared to the 0.6% mix, although it remained higher than that of the control concrete. This reduction could be attributed to less efficient fiber distribution at higher contents, which may limit the fibers' beneficial contribution to tensile strength.

Mechanical results showed varying trends depending on the PALF dosage. Compressive and splitting tensile strengths increased progressively up to a PALF dosage of 0.6%, after which both properties declined at the 0.8% level. Compared to the 0.6% mix, the 0.8% mix exhibited reductions of approximately 9.87% and 14.15% in compressive strength at 7 and 28 days, respectively, while splitting tensile strength decreased by approximately 1.95% and 1.69%. In contrast, flexural strength continued to increase across the entire range of PALF dosages evaluated, reaching its peak value at 0.8%. These results indicate that the PALF dosage yielding the highest flexural strength was not the same as the one providing the most favorable overall balance of mechanical properties. Similar dosage-dependent trends have been reported for other fiber-reinforced concretes, where excessive fiber content can negatively affect certain mechanical properties [48]. As depicted in Figure 19(a) and Figure 19(b) that qualitative show visible PALF fibers going remain through fissured and cracked surfaces of the specimens after the test.

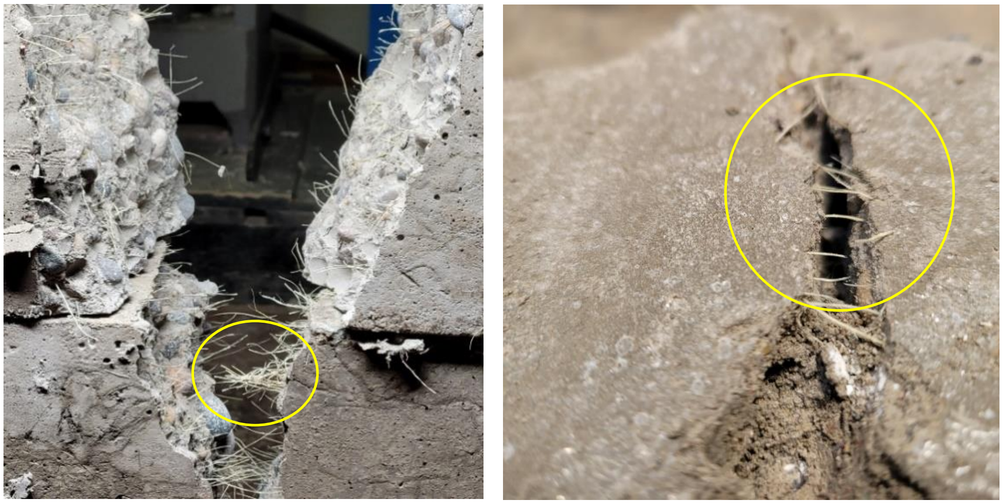

(a) **(b)**

Fig. 20 Evidencia visual cualitativa de fibras de PALF atravesando superficies fisuradas y fracturadas del concreto después de los ensayos mecánicos: (a) vista cercana de fibras de PALF atravesando una fisura, (b) Probetas de concreto fracturadas con fibras de PALF visibles a través de las superficies de falla.

Although qualitative photographic evidence of visible fibers on the fissured and fractured surfaces was obtained, no systematic or quantitative characterization of the failure patterns was performed. Likewise, microstructural characterization via SEM/EDX, load-deflection curves, residual strength, crack width measurements, and flexural toughness were not included in the experimental program; the mechanical evaluation was based primarily on peak strength measurements. Therefore, interpretations regarding fiber-matrix adhesion, crack bridging, fiber agglomeration, and post-cracking mechanisms should be considered as literature-supported explanations for the observed mechanical trends, rather than as direct experimental evidence from the present study. Future research should incorporate microstructural characterization and post-cracking measurements to directly verify these mechanisms and provide a more comprehensive evaluation of PALF-reinforced concrete.

4.1. Sustainability and Economic Analysis of PALF

The use of PALF fiber shows suitable results for its integration into concrete, since it presents optimal values similar to those reported for steel, polypropylene, coconut, and sisal fibers. This comparison helps to better understand the use of fibers in relation to the behavior and properties of concrete in the fresh state, as well as its mechanical performance in the hardened state. Through this, it is possible to identify the advantages and disadvantages of these fibers in comparison with PALF.

Table 11. Comparison of natural fibers with PALF

Fiber	Author(es)	Main reported result	Comparison with PALF
PALF	Abisha and Nalanth (2023)[25]	The author found that PALF fiber reduced workability by 0.2%, but compressive strength and indirect tensile strength improved.	A standard dosage should be maintained for better performance.
PALF / Polypropylene	Hendrian et al. (2021) [9]	The author found that both fibers changed the fluidity of concrete, but increased its mechanical properties. PP showed slightly higher mechanical values in some dosages.	Compared with PP, PALF shows improvements and also has the additional advantage of being a natural and renewable fiber.
PALF	Hasan et al. (2026) [13]	PALF concentrations ranging from 1% to 4% were evaluated, with the 2% concentration showing the best overall performance. SEM/EDX analyses confirmed improved fiber-matrix interaction at the optimal dosage, and cost and CO_2 emission assessments were also conducted.	evaluated a higher PALF dosage range and included microstructural and sustainability analyses, whereas the present study focuses on PALF concentrations of 0.2% to 0.8% and a detailed evaluation of fresh-state mobility, passing ability, and mechanical strength.

Steel	Alberti et al. (2014)[49]	The author found that steel fiber obtained a better response in compressive and tensile tests.	Compared with PALF, steel has higher mechanical efficiency.
Coconut	Ahmad et al. (2020)[16]	The author found that coconut fiber improved indirect tensile strength and flexural strength.	Coconut fiber and PALF show similar behavior due to their lignocellulosic nature, since both components have similar characteristics.
Sisal	Okeola et al. (2018)[50]	The author found that sisal fiber considerably reduced slump, but intermediate contents improved indirect tensile strength.	Sisal fiber and PALF have similar characteristics: lower workability but improved tensile behavior when an appropriate amount is used.

Based on the research, it can be observed that PALF fiber has favorable impacts when used as an additive in concrete mixtures. It not only helps to improve mechanical properties, but also supports the reuse of organic waste, since pineapple leaves are usually considered a material with little use or relevance. Their use in concrete mixtures can help to promote the use of agricultural additives and support the reuse of these residues [8]. It is known that pineapple leaves were used to make ropes or alternative materials, but this reuse was done on a smaller scale and with relatively low prices. Now, with their use in concrete mixtures, their value could increase and become an indirect source of income for agricultural producers [51]. However, this process or the creation of new forms of reuse for pineapple leaves does not guarantee a reduction in the environmental footprint. When PALF is integrated into concrete, greater care is required by farmers to obtain suitable fiber for use in concrete mixtures. The production of PALF requires energy and chemical treatments, so these factors must be considered in a more complete life cycle assessment [26]. The use of PALF fiber for reducing environmental impacts or improving waste use will depend on both the type of residue and the efficiency of the process used to obtain the fiber. It is known that the use of PALF fiber benefits concrete mixtures and can also help improve the economy of the agricultural sector. However, its production will require greater commitment from the stakeholders involved. With a good dosage and an adequate PALF fiber, suitable results can be obtained for both sides.

Considering the importance of PALF fiber compared with new construction materials, both in waste reduction and indirect economic generation, PALF has a special characteristic because it is hydrophilic. Some studies have found water absorption increases of up to 150%. This effect can be useful for the curing process of concrete and may reduce the use of additives or concrete curing compounds, but this should be considered with an adequate or optimal dosage in order to make better use of these characteristics [8, 52] . Based on this, care must be taken when using PALF fiber or other fibers, especially at higher percentages. PALF fiber can improve the durability of mortar or concrete when treated with 6% NaOH, as long as an adequate dosage is considered [53, 54].

5. Conclusion

The results showed that the incorporation of PALF caused progressive changes in the properties of the concrete in both its fresh and hardened states. In mixtures without superplasticizer, the slump decreased from 74 mm in the control mix to 49 mm with a 0.8% PALF dosage, demonstrating a reduction in workability as fiber content increased. Air content dropped from 1.90% in the control mix to 1.47% with 0.6% PALF, then rose to 1.57% with 0.8%, indicating a dosage-dependent variation.

In mixtures containing superplasticizer, the slump-flow decreased progressively from 699 mm in the control mix to 620 mm with 0.8% PALF. J-Ring and L-box tests revealed that mixtures with fiber contents between 0% and 0.4% maintained adequate passing ability; however, the mixture with 0.6% PALF approached the acceptance limit, and the mixture with 0.8% showed a more pronounced reduction in passing ability. These results confirm that increasing PALF content progressively reduces the mobility of fresh concrete within the range evaluated.

In the hardened state, the 0.6% PALF dosage yielded the highest values for compressive strength and splitting tensile strength. Compared to the control mix, this dosage increased compressive strength by 13.45% at 7 days and 22.32% at 28 days, while splitting tensile strength increased by 29.48% and 37.42%, respectively. For its part, flexural strength increased progressively across the entire range studied, reaching its maximum value at 0.8% PALF, with increases of 23.32% at 7 days and 23.34% at 28 days compared to the control concrete.

When considering both fresh and hardened state properties, the 0.6% PALF dosage was identified as the most favorable condition within the evaluated range, as it provided the best overall balance among workability, passing ability, compressive strength, and splitting tensile strength. Although the 0.8% dosage yielded the highest flexural strength, it also resulted in the most significant reduction in fluidity and passing ability. Therefore, the results indicate that the optimal dosage depends on the performance criterion considered, with 0.6% representing the most balanced alternative for the experimental conditions studied.

It should be noted that this study was primarily limited to evaluating fresh-state properties and peak mechanical strengths. No microstructural analyses, crack width measurements, load-deflection curves, residual strength assessments, or toughness tests were conducted. Consequently, fiber-matrix interaction mechanisms and post-cracking behavior cannot be directly determined from the obtained results. Future research should incorporate these evaluations to complement the characterization of PALF-reinforced concrete.

References

[1] Olajesu Olanrewaju, Isiaka Oluwole Oladele, and Samson Oluwagbenga Adelani, "Natural Fiber Biocomposites: A Comprehensive Review of Current Developments and Material Properties of Plant and Animal Fiber Reinforcements in Cement Concrete, and Ultra-High-Performance Concrete," *Next Materials*, vol. 9, pp. 1-35, 2025. [CrossRef] [Google Scholar] [Publisher Link]

[2] B.G.V. Sanjaya et al., "Enhancing Structural Integrity and Crack Resistance of Rubberized Concrete using Aqua-Thermally Treated Rubber Aggregates and Recycled Tire Steel Fibers for Structural Applications," *Sustainable Materials and Technologies*, vol. 46, pp. 1-25, 2025. [CrossRef] [Google Scholar] [Publisher Link]

[3] Comptroller's Office Warns of Cracks and Fissures in San Juan de la Virgen Bridge, Office of the Comptroller General of the Republic, 2025. [Online]. Available: https://www.gob.pe/institucion/contraloria/noticias/1255407-contraloria-advierte-presencia-de-fisuras-y-grietas-en-puente-de-san-juan-de-la-virgen

[4] Ai-Hua Jin et al., "Influence of Concrete Strength and Fiber Properties on Residual Flexural Strength of Steel Fiber-Reinforced Concrete," *Construction and Building Materials*, vol. 489, pp. 1-19, 2025. [CrossRef] [Google Scholar] [Publisher Link]

[5] Federico Ponsi et al., "Temperature Effect on the Tensile Constitutive Parameters of Fiber Reinforced Concrete," *Construction and Building Materials*, vol. 501, pp. 1-15, 2025. [CrossRef] [Google Scholar] [Publisher Link]

[6] Osama Zaid et al., "State of the Art Review on Ultra-High-Performance Fiber Reinforced Concrete Properties Standardization and Structural Applications," *Discover Sustainability*, vol. 7, no. 1, pp. 1-53, 2025. [CrossRef] [Google Scholar] [Publisher Link]

[7] Gejun Tong et al., "Study on the Durability and Mechanical Properties of Carbon Fiber Reinforced Concrete for Shaft Lining Under Chloride Salt Freeze–Thaw Coupling Environment," *Scientific Reports*, vol. 16, no. 1, pp. 1-23, 2026. [CrossRef] [Google Scholar] [Publisher Link]

[8] Julianna M. da Silva et al., "Characterization and Application of Different Types of Pineapple Leaf Fibers (PALF) in Cement-Based Composites," *Fibers*, vol. 13, no. 5, pp. 1-20, 2025. [CrossRef] [Google Scholar] [Publisher Link]

[9] Hanoora Sarah Anindita Hendrian et al., "Physical and Mechanical Properties of Self-Compacting Concrete (SCC) with Pineapple Leaf Fibre and Polypropylene," *Journal of Physics: Conference Series: Journal of Physics: Conference Series, Volume 1783, Annual Conference on Science and Technology Research (ACOSTER)*, Medan, Indonesia, vol. 1783, no. 1, pp. 1-7, 2021. [CrossRef] [Google Scholar] [Publisher Link]

[10] Cunmiao Gao et al., "Experimental Study on Flexural Behaviors and Theoretical Compression-Bending Capacity of Unreinforced Steel Fiber Reinforced Concrete," *Buildings*, vol. 15, no. 7, pp. 1-28, 2025. [CrossRef] [Google Scholar] [Publisher Link]

[11] Shuhao Qin, and Liao Wu, "Study on Mechanical Properties and Mechanism of New Basalt Fiber Reinforced Concrete," *Case Studies in Construction Materials*, vol. 22, pp. 1-13, 2025. [CrossRef] [Google Scholar] [Publisher Link]

[12] Yulieth Manuela Delgado Zambrano, and Yuri Camilo Delgado Benavides, "Potential Regions for the use of Natural Fibres in Building Materials," *International Engineering Education Meeting ACOFI 2023*, pp. 1-10, 2023. [CrossRef] [Google Scholar] [Publisher Link]

[13] Noor Md. Sadiqul Hasan et al., "Sustainable Fiber-Reinforced Concrete: Assessing Pineapple Leaf Fiber as a Green Reinforcement Material," *Australian Journal of Civil Engineering*, pp. 1-23, 2026. [CrossRef] [Google Scholar] [Publisher Link]

[14] Ali Jahami, Nour Zeaiter, and Mounir Cheaib, "Reviewing the Potential: A Comprehensive Review of Natural Fibers (NFs) in Structural Concrete and their Multifaceted Influences," *Innovative Infrastructure Solutions*, vol. 9, 2024. [CrossRef] [Google Scholar] [Publisher Link]

[15] Mohammed A. Abed et al., "Influence of Polypropylene and Steel Fibers on the Performance and Crack Repair of Self-Compacting Concrete," *Materials*, vol. 14, no. 19, pp. 1-15, 2021. [CrossRef] [Google Scholar] [Publisher Link]

[16] Waqas Ahmad et al., "Effect of Coconut Fiber Length and Content on Properties of High Strength Concrete," *Materials*, vol. 13, no. 5, pp. 1-22, 2020. [CrossRef] [Google Scholar] [Publisher Link]

[17] *ASTM C150/C150M – Standard Specification for Portland Cement*, ASTM International, pp. 1-8, 2007. [CrossRef] [Publisher Link]

[18] Steven H. Kosmatka, William C. Panarese, and Beatrix Kerkhoff, *Design and Control of Concrete Mixtures*, Portland Cement Association, pp. 1-358, 2002. [Google Scholar] [Publisher Link]

[19] *ASTM C136/C136M-19: Standard Test Method for Sieve Analysis of Fine and Coarse Aggregates*, ASTM International, pp. 1-5, 2019. [CrossRef] [Google Scholar] [Publisher Link]

[20] *ASTM C127-24: Standard Test Method for Relative Density (Specific Gravity) and Absorption of Coarse Aggregate*, ASTM International, pp. 1-6, 2024. [CrossRef] [Google Scholar] [Publisher Link]

[21] *ASTM C128-22 Standard Test Method for Relative Density (Specific Gravity) and Absorption of Fine Aggregate*, ASTM International, pp. 1-6, 2022. [CrossRef] [Google Scholar] [Publisher Link]
[22] *ASTM C29/C29M-23: Standard Test Method for Bulk Density ("Unit Weight") and Voids in Aggregate*, ASTM International, pp. 1-5, 2023. [CrossRef] [Google Scholar] [Publisher Link]
[23] *ASTM C494/C494M-24 Standard Specification for Chemical Admixtures for Concrete*, ASTM International, pp. 1-15, 2024. [Google Scholar] [Publisher Link]
[24] *ASTM C1602/C1602M-22 Standard Specification for Mixing Water Used in the Production of Hydraulic Cement Concrete*, ASTM International, pp. 1-5, 2022. [CrossRef] [Google Scholar] [Publisher Link]
[25] Yesudhas Abisha, and Natarajan Nalanth, "Pineapple Fibre as an Additive to Self-Compacting Concrete," *Matter (Rio de Janeiro)*, vol. 28, no. 1, pp. 1-8, 2023. [Google Scholar] [Publisher Link]
[26] Huy N. Q. Phan et al., "Rapid Fabrication of Pineapple Leaf Fibers from Discarded Leaves by Using Electrolysis of Brine," *Textiles*, vol. 3, no. 1, pp. 1-10, 2023. [CrossRef] [Google Scholar] [Publisher Link]
[27] Alejandro Flores Nicolás et al., "Mechanical Behavior of Concrete Reinforced with Natural Palm and Mango Fibers," *Journal of Engineering and Technological Sciences*, vol. 57, no. 1, pp. 48-65, 2025. [CrossRef] [Google Scholar] [Publisher Link]
[28] *ASTM C192/C192M: Standard Practice for Making and Curing Concrete Test Specimens in the Laboratory*, ASTM International, pp. 1-9, 2026. [CrossRef] [Google Scholar] [Publisher Link]
[29] *ACI PRC-211.1-22: Selecting Proportions for Normal-Density and High Density-Concrete – Guide*, American Concrete Institute, pp. 1-38, 2022. [Google Scholar] [Publisher Link]
[30] *ASTM C143/C143M-20: Standard Test Method for Slump of Hydraulic-Cement Concrete*, ASTM International, pp. 1-4, 2020. [CrossRef] [Google Scholar] [Publisher Link]
[31] *ASTM C138/C138M-17a: Standard Test Method for Density (Unit Weight), Yield, and Air Content (Gravimetric) of Concrete*, ASTM International, pp. 1-6, 2017. [CrossRef] [Google Scholar] [Publisher Link]
[32] *ASTM C231/C231M-22: Standard Test Method for Air Content of Freshly Mixed Concrete by the Pressure Method*, ASTM International, pp. 1-10, 2022. [CrossRef] [Google Scholar] [Publisher Link]
[33] NTP 339.080: Pressure Method for Determining Air Content in Concrete, 2020. [Online]. Available: https://www.studocu.com/pe/document/universidad-peruana-de-ciencias-aplicadas/tecnologia-del-concreto/ntp-339080-metodo-de-presion-para-determinar-contenido-de-aire-en-concreto/138008692?sid=ea3796fa-6dd1-4538-8889-1ee801754a201790328993
[34] *ASTM C1611/C1611M-21: Standard Test Method for Slump Flow of Self-Consolidating Concrete*," ASTM International, pp. 1-16, 2021. [CrossRef] [Publisher Link]
[35] *ASTM C1621/C1621M-14 Standard Test Method for Passing Ability of Self-Consolidating Concrete by J-Ring*, ASTM International, pp. 1-5, 2014. [CrossRef] [Publisher Link]
[36] European Committee for Standardization, *BS EN 12350-10:2010 Testing fresh Concrete - Self-Compacting Concrete. L Box Test*, BSI, 2010. [Publisher Link]
[37] *ASTM C39/C39M-23 Standard Test Method for Compressive Strength of Cylindrical Concrete Specimens*, ASTM International, pp. 1-8, 2023. [CrossRef] [Publisher Link]
[38] *NTP 339:2015 - Standard Test Method for Determining the Compressive Strength of Concrete in Cylindrical Samples*, Peruvian Technical Standards, 2015. [Google Scholar] [Publisher Link]
[39] *ASTM C496/C496M: Standard Test Method for Splitting Tensile Strength of Cylindrical Concrete Specimens*, ASTM International, 2004. [CrossRef] [Google Scholar] [Publisher Link]
[40] *ASTM C78/C78M-18 Standard Test Method for Flexural Strength of Concrete (Using Simple Beam with Third-Point Loading)*, ASTM International, pp. 1-5, 2018. [CrossRef] [Google Scholar] [Publisher Link]
[41] Qunyi Huang et al., "Research on the Workability of 3D Printed Fiber-Reinforced Concrete Materials," *Fibers*, vol. 14, no. 1, pp. 1-14, 2026. [CrossRef] [Google Scholar] [Publisher Link]
[42] Aris Aryanto, and Andy Muliohardjo, "Effect of Macro-Synthetic Polypropylene Fiber on Mechanical Properties and Drying Shrinkage Cracking of Self-Consolidating Concrete," *International Journal of Geomate*, vol. 24, no. 101, pp. 60-67, 2023. [Google Scholar] [Publisher Link]
[43] Lucas Onghero et al., "Influence of Glass Microfibers on the Control of Autogenous Shrinkage in Very High Strength Self-Compacting Concretes (VHSSCC)," *Journal of Composites Science*, vol. 8, no. 3, pp. 1-16, 2024. [CrossRef] [Google Scholar] [Publisher Link]
[44] Ahmed Redha Abdul-Rahman, Khaleel Hasan Younis, and Bahman Omar Taha, "Interactive Influence of Recycled Concrete Aggregate and Recycled Steel Fibers on the Fresh and Hardened Performance of Eco-Efficient Fiber-Reinforced Self-Compacting Concrete," *Journal of Composites Science*, vol. 10, no. 1, pp. 1-19, 2025. [CrossRef] [Google Scholar] [Publisher Link]
[45] Ali Ejaz et al., "Development of Nano-Calcium Carbonate-Modified Green Self-Compacting Concrete Incorporating Recycled Tempered Glass and Waste Cotton Rope Fibers," *Journal of Building Engineering*, vol. 117, 2026. [CrossRef] [Google Scholar] [Publisher Link]

[46] Thong M. Pham, “Fibre-Reinforced Concrete: State-of-the-art-review on Bridging Mechanism, Mechanical Properties, Durability, and Eco-Economic Analysis,” *Case Studies in Construction Materials*, vol. 22, pp. 1-46, 2025. [CrossRef] [Google Scholar] [Publisher Link]

[47] Mohammed Abdulkareem Adisa, Samuel Oshadare, and Yassar Yusuf, “Mechanical Properties of Fiber-Reinforced Concrete Using Steel Fibers Derived from Discarded Tires,” *International Journal of Concrete Structures and Materials*, vol. 20, no. 1, pp. 1-8, 2026. [CrossRef] [Google Scholar] [Publisher Link]

[48] Shibo Bao et al., “Enhancing the Mechanical Properties of Recycled Aggregate Concrete: A Comparative Study of Basalt- and Glass-Fiber Reinforcements,” *Buildings*, vol. 15, no. 10, pp. 1-31, 2025. [CrossRef] [Google Scholar] [Publisher Link]

[49] Marcos García Alberti, Alejandro Enfedaque Díaz, and Jaime C. Gálvez Ruiz, “Self-Compacting Concrete Simultaneously Reinforced with Structural Polyolefin Fibers and Shaped Steel Fibers,” *Cement and Concrete*, no. 963, 2014. [Google Scholar] [Publisher Link]

[50] Abass Abayomi Okeola, Silvester Ochieng Abuodha, and John Mwero, “Experimental Investigation of the Physical and Mechanical Properties of Sisal Fiber-Reinforced Concrete,” *Fibers*, vol. 6, no. 3, pp. 1-16, 2018. [CrossRef] [Google Scholar] [Publisher Link]

[51] Clara Yuqi Liao, Ysabel Jingyi Guan, and Mauricio Bustamante-Román, “Techno-Economic Analysis and Life Cycle Assessment of Pineapple Leaves Utilization in Costa Rica,” *Energies*, vol. 15, no. 16, pp. 1-13, 2022. [CrossRef] [Google Scholar] [Publisher Link]

[52] Kaiyue Zhao et al., “Application of Natural Plant Fibers in Cement-Based Composites and the Influence on Mechanical Properties and Mass Transport,” *Materials*, vol. 12, no. 21, pp. 1-16, 2019. [CrossRef] [Google Scholar] [Publisher Link]

[53] Bebitta Robinson Chellathurai, and Ninija Merina Rymond, “Durability Evaluation of Treated Pineapple Leaf Biopolymer Composites for Enhanced Eco-Friendly Mortar Towards Sustainability,” *Biomass Conversion and Biorefinery*, vol. 14, no. 8, pp. 9897-9913, 2024. [CrossRef] [Google Scholar] [Publisher Link]

[54] M.D. de Klerk et al., “Durability of Chemically Modified Sisal Fibre in Cement-based Composites,” *Construction and Building Materials*, vol. 241, 2020. [CrossRef] [Google Scholar] [Publisher Link]